codon. The same probes were used to identify targeted clones and genotyping.
10. N. Ben-Arie *et al.*, in preparation.
11. Pregnant females were culled, and embryos were dissected in ice-cold phosphate-buffered saline (PBS). The surrounding yolk sac was collected for genotyping. Embryos were fixed for 30 min in 4% paraformaldehyde/PBS then incubated in X-Gal (1 mg/ml) at 30°C for revealing β-Gal activity. Stained embryos were washed in PBS, postfixed for 1 hour in 4% paraformaldehyde/PBS, dehydrated, and either embedded in paraffin before sectioning or dissected to remove the inner ear for whole-mount studies.
12. N. A. Bermingham *et al.*, unpublished data.
13. LM and TEM were carried out as previously described (*29*). Tissue preparation for SEM consisted of treatment with 1% OsO_4 in cacodylate buffer, dehydration, critical-point drying, sputter coating with gold, and examination in a JEOL 35S electron microscope.
14. A. Rüsch, A. Lysakowski, R. A. Eatock, *J. Neurosci.* **18**, 7487 (1998).
15. M. Xiang *et al.*, *Proc. Natl. Acad. Sci. U.S.A.* **94**, 9445 (1997).
16. M. Xiang, W. Q. Gao, T. Hasson, J. J. Shin, *Development* **125**, 3935 (1998).
17. T. Hasson *et al.*, *J. Cell Biol.* **137**, 1287 (1997).
18. C. J. Dechesne, D. Rabejac, G. Desmadryl, *J. Comp. Neurol.* **346**, 517 (1994).
19. J. L. Zheng and W. Q. Gao, *J. Neurosci.* **17**, 8270 (1997).
20. For immunofluorescence, embryos were fixed for 1.5 hours in 4% paraformaldehyde/PBS at 4°C, sunk through 15% sucrose/PBS for 5 hours then through 30% sucrose/PBS overnight, and snap frozen in a 2-methylbutane dry ice bath. Fourteen-micrometer sections were cut on a cryostat and mounted on gelatin-coated slides. Sections were fixed on slides by dipping for 10 min in Streck tissue fixative (Streck Laboratories, Omaha, NE) and air drying. Sections were blocked in 10% normal goat serum and 0.3% Triton X-100 in PBS for 1 hour at room temperature (RT). Rabbit polyclonal antibody to calretinin (Chemicon International, Temecula, CA) was diluted 1:200 or rabbit antibody to myosin VI (a gift from T. Hasson, University of California, San Diego) was diluted 1:100 in blocking solution and incubated overnight on sections at 4°C. Sections were washed three times (20 min each) in PBS at RT. The secondary antibody, Alexa 488 (Molecular Probes, Eugene, OR), was diluted 1:400 in blocking solution. Sections were covered and incubated at RT for 2 hours before washing and mounting in Vectashield containing 4′6′-diamidino-2-phenylindole (DAPI) (Vector Laboratories, Burlingame, CA). For confocal microscopy, sections were treated with ribonuclease (25 μg/ml) before counterstaining with propidium iodide (50 μg/ml) and mounted in Vectashield without DAPI or were directly mounted in Vectashield containing TOTO-3 iodide (Molecular Probes). Stained sections were viewed under a Bio-Rad 1024 confocal microscope.
21. G. M. Cohen and C. D. Fermin, *Hear. Res.* **18**, 29 (1985).
22. M. J. Shiel and D. A. Cotanche, *ibid.* **47**, 147 (1990).
23. A. P. Jarman, Y. Grau, L. Y. Jan, Y. N. Jan, *Cell* **73**, 1307 (1993).
24. D. Eberl, personal communication.
25. B. A. Hassan and H. J. Bellen, unpublished observations.
26. C. Haddon, Y. J. Jiang, L. Smithers, J. Lewis, *Development* **125**, 4637 (1998); J. Adam *et al.*, *ibid.* **125**, 4645 (1998); P. Lanford *et al.*, *Nature Genet.* **21**, 289 (1999).
27. P. Kim, A. W. Helms, J. E. Johnson, K. Zimmerman, *Dev. Biol.* **187**, 1 (1997).
28. G. Friedrich and P. Soriano, *Genes Dev.* **5**, 1513 (1991).
29. A. Lysakowski and J. M. Goldberg, *J. Comp. Neurol.* **389**, 419 (1997)
30. We thank R. Atkinson, D. Trikka, and V. Brandt for assistance and helpful discussions and T. Hasson for the myosin VI antibody, and we acknowledge the support of the Electron Microscopic Facility of the University of Illinois Research Resources Center. N.A.B. and B.A.H. are associate fellows, H.J.B. is an Associate Investigator, and H.Y.Z. is an Investigator with the Howard Hughes Medical Institute. This work was partially supported by a grant from the National Institute on Deafness and Other Communication Disorders to R.A.E. and A.L. and by cores of the Mental Retardation Research Center at the Baylor College of Medicine.

14 December 1998; accepted 10 May 1999

Crystal Structure of the Zα Domain of the Human Editing Enzyme ADAR1 Bound to Left-Handed Z-DNA

Thomas Schwartz,[1] Mark A. Rould,[2] Ky Lowenhaupt,[1] Alan Herbert,[1] Alexander Rich[1]*

The editing enzyme double-stranded RNA adenosine deaminase includes a DNA binding domain, Zα, which is specific for left-handed Z-DNA. The 2.1 angstrom crystal structure of Zα complexed to DNA reveals that the substrate is in the left-handed Z conformation. The contacts between Zα and Z-DNA are made primarily with the "zigzag" sugar-phosphate backbone, which provides a basis for the specificity for the Z conformation. A single base contact is observed to guanine in the syn conformation, characteristic of Z-DNA. Intriguingly, the helix-turn-helix motif, frequently used to recognize B-DNA, is used by Zα to contact Z-DNA.

Since the elucidation of the structure of left-handed Z-DNA in 1979 (*1*), the question of a biological role for this conformation has remained in the forefront of research in the field. The discovery of a Z-DNA binding activity for double-stranded (ds) RNA adenosine deaminase (ADAR1) constituted an important step (*2*). ADAR1 deaminates adenine in pre-mRNA, yielding inosine, which codes as guanine. Such codon changes result in alternative forms of the translated protein. The NH_2-terminus of ADAR1 includes a domain, Zα, which is responsible for high-affinity binding to the Z conformation of DNA. This was originally shown by a band-shift assay (*3*), where the binding withstood a challenge of a 10,000-fold mass excess of nonspecific B-DNA competitor (*2, 4*). Circular dichroic and Raman spectroscopic measurements have confirmed the specificity of Zα containing peptides for Z-DNA (*4–6*). Zα is the prototype for a family of related peptides, which share common amino acid sequence motifs (*4*). We have now cocrystallized a proteolytically defined Zα domain [residues 133 to 209 (*7, 8*)] of human ADAR1 with the 6–base pair (bp) DNA fragment $d(TCGCGCG)_2$. The structure was determined by single isomorphous replacement including anomalous scattering (SIRAS) and was refined to a resolution of 2.1 Å (Table 1).

The monomeric Zα domain binds to one strand of the palindromic dsDNA. The conformation of the DNA substrate is very similar to the canonical Z-DNA structure determined by Wang *et al.* (*1, 9*) [root mean square deviation (rmsd) 0.80 Å, including all atoms in the duplex]. A second monomer related by the twofold axis of the DNA oligomer binds to the opposite strand of the DNA; however, the two proteins do not interact with each other. In the asymmetric unit there are three independent Zα-DNA complexes (*10*).

The Zα domain has a compact α/β architecture containing a three-helix bundle (α1 to α3) flanked on one side by a twisted antiparallel β sheet (β1 to β3) (Fig. 1). The NH_2-terminal helix α1 (Ser^{134} to Leu^{150}) is followed by the short-strand β1 (Ala^{155} to Thr^{157}), which positions the COOH-terminal β hairpin (β2: Leu^{185} to Ala^{188}; β3: Pro^{193} to Ile^{197}) by means of two hydrogen bonds. This arrangement of a β hairpin with exactly two hydrogen bonds to a third β strand is a common feature of helix-turn-helix (HTH) proteins with α/β topology. Helices α2 and α3 (Ala^{158} to Leu^{165} and Lys^{169} to Lys^{182}) reside between β1 and β2 and form the HTH motif. Aliphatic residues from the three helices, together with Trp^{195} in strand β3, interdigitate and form a hydrophobic core. The secondary structure reported in a nuclear magnetic resonance experiment indicates that the unbound protein in solution adopts a very similar fold (*11*).

[1]Department of Biology, Massachusetts Institute of Technology, Cambridge, MA 02139, USA. [2]Department of Molecular Physiology and Biophysics, University of Vermont, Burlington, VT 05405, USA.

*To whom correspondence should be addressed.

The contact between Zα and the DNA strand consists of a single continuous recognition surface (Fig. 2). This surface, which is complementary to the DNA in terms of shape and electrostatic nature, consists of residues from helix α3 and the COOH-terminal β hairpin. All the polar interactions in the complex are with the sugar-phosphate backbone. Direct contacts are made between Lys^{169}, Lys^{170}, Asn^{173}, Arg^{174}, and Tyr^{177} in helix α3 as well as Thr^{191} and five consecutive phosphates. In addition water-mediated phosphate contacts are observed. Lys^{169}, Asn^{173}, and Trp^{195} coordinate two ordered water molecules embedded within the protein-DNA interface in all three independent complexes. These waters are completely shielded from the surface. Further, Thr^{191} and Arg^{174} also bind to the furanose oxygens of G2 and G6, respectively. This ensemble of residues forms an extensive network of hydrogen bonds; four of the five consecutive phosphate groups are grasped by at least two hydrogen bond donors.

In concert with these polar interactions, the crystal structure reveals a striking complementarity in the van der Waals surfaces of the protein and the DNA. Peptide backbone atoms of helix α3 (Lys^{170}, Arg^{174}) contact the ribose of G4. The face of the aromatic ring of Tyr^{177} makes a close van der Waals contact with the exposed carbon 8 of G4. This interaction is possible only if this base is in the syn conformation and is therefore specific for Z-DNA. The phenolic side chain of Tyr^{177} is almost perpendicular to the G4 base. Further, the aromatic ring of Trp^{195} is perpendicular to the Tyr^{177} ring from the other side and buttresses it from within the protein core. Similar systems of mutually perpendicular aromatic rings in an edge-to-face orientation have been shown to stabilize other protein-ligand interactions (*12*). In Zα, Trp^{195}, positioned precisely within the hydrophobic core, maintains two important indirect DNA contacts, via Tyr^{177} and via a water to the backbone. This central role of Trp^{195} explains the detrimental effect of Trp^{195} to Ala (W195A) and Trp^{195} to Tyr (W195Y) mutations (*13*) on both protein stability and DNA binding as well as the tryptophan fluorescence quenching observed as a result of Z-DNA binding (*5, 11*).

Pro^{192} and Pro^{193} in the COOH-terminal β-hairpin form another important van der Waals interaction with the DNA. The pyrrolidine rings of both residues pack against the sugar-phosphate backbone from phosphate 2 to phosphate 3. In contrast to the predominant trans peptide linkage, Pro^{192} forms a cis peptide bond, thereby positioning the β-hairpin loop against the DNA surface. The absolute conservation of Pro^{192} within the known homologues of Zα (*4*) underlines the importance of this local structure.

Finally, an array of well-defined waters is positioned on the edge of the protein-DNA interface. The total structure, including this bonded water network on the protein-DNA interface, is nearly identical in all three inde-

Table 1. Crystallographic data. Recombinant Zα (residues 133 to 209 of hADAR1) was overproduced and purified from *Escherichia coli* as described (*7*). Single crystals of the protein-DNA complex were obtained by the hanging-drop vapor diffusion method with ammonium sulfate used as precipitant [for details see (*26*)]. The crystals belong to space group $P42_12$ with cell dimensions $a = b = 85.9$ Å, $c = 71.3$ Å. Three protein-DNA complexes form the asymmetric unit. Derivatives were prepared by substituting 5-iodouracil for thymine 1 (iodo-1) and 5-iodocytosine for cytosine 6 (iodo-6), although only the latter served as a suitable derivative. Diffraction data were collected from cryocooled crystals on a rotating anode x-ray source with an R-Axis IIc image plate detector and reduced with the HKL program package (*20*). Iodine sites were located and initial SIRAS phases were calculated with SOLVE (*20*). Solvent flattening and noncrystallographic symmetry (NCS) averaging with DM (*20*) gave a readily interpretable electron density map. Because the iodo-1 derivative diffracted to higher resolution than the original native, it was used for model building and refinement with X-PLOR (*20*). NCS restraints were not used during refinement, and water molecules were added to the three complexes independently. A total of 158 of 161 nonglycine residues lie in most-favored regions of the Ramachandran plot. The remaining three residues lie in additional favored regions [calculated with Procheck (*20*)].

Data collection and SIRAS phasing statistics

	Native	Iodo-1	Iodo-6
DNA	d(TCGCGCG)	d(^{5I}UCGCGCG)	d(TCGCG^{5I}CG)
Data coverage (Å)	40–2.4	20–2.1	20–2.8
R_{merge}* (%)	5.2	7.4	12.0
Number of unique reflections	10896	29702	12566
Completeness (%)	99.2	99.9	99.9
Redundancy	6.6	9.8	6.9
R_{iso}† (%)	—	—	22.3
R_{Cullis}‡ (%)	—	—	57.0
Iso. phasing power§	—	—	1.34
Anom. phasing power	—	—	1.06
Figure of merit, SIRAS	0.490		
Figure of merit, DM	0.822		

Refinement statistics (6–2.1 Å)

			Protein	DNA	Water
R_{cryst}¶ (%)	22.7				
R_{free}¶ (%)	26.5	rms from ideality:			
Reflections in working set	13772	Bond lengths (Å)	0.006	0.004	
Reflections in test set	1531	Bond angles (°)	1.12	0.67	
N_{atoms}	1898	Average B-factor (Å^2)	32.9	21.9	43.0
N_{waters}	244	rms B-factors‖ (Å^2)	3.31	3.19	

*$R_{merge} = \Sigma_i|I_h - I_{h,i}|/\Sigma_i I_{h,i}$, where I_h is the mean intensity for the reflection. †$R_{iso} = \Sigma|F_{PH} - F_P|/\Sigma F_P$. ‡$R_{Cullis} = \Sigma||F_{PH} \pm F_P| - F_{H\ calc}|/\Sigma|F_{PH} \pm F_P|$ for centric reflections only. §Phasing power = rms($F_{H(calc)}$)/rms (phase-integrated lack of closure). ¶$R_{cryst} = \Sigma|F_P - F_{P(calc)}|/\Sigma F_P$. R_{free} is the same as R_{cryst} but calculated on 10% of data selected evenly over the resolution range and excluded from refinement. ‖Between covalently bonded atoms.

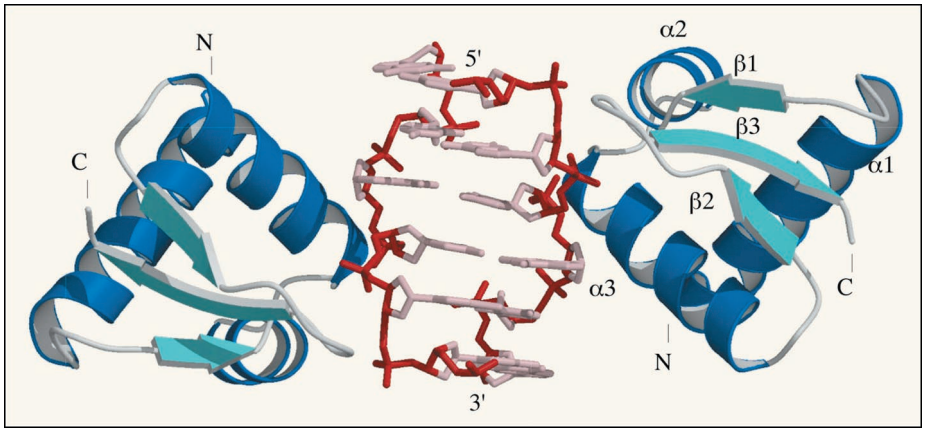

Fig. 1. Overview of the Zα domain bound to left-handed Z-DNA. Residues 134 to 198 of two symmetry-related Zα monomers and the 6-bp DNA duplex $d(CGCGCG)_2$ are shown. Labels indicate NH_2- (N) and COOH-termini (C) of the proteins as well as helices (α1 to α3) and strands (β1 to β3) (*27*).

pendent complexes in the asymmetric unit (*14*).

Zα belongs to the family of HTH proteins with α/β topology (*15*) (Fig. 3C). The interaction of HTH proteins with right-handed DNA has been well characterized. Typically, the second helix of the HTH motif, called the recognition helix, is cradled in the major groove. There, the base edges expose a characteristic pattern of potential hydrogen bond donors and acceptors, which allow for base-specific recognition. In the family of HTH proteins with α/β topology, DNA contacts are also made between residues in the first helix of the HTH motif and the phosphate backbone. In variants of the family, additional contacts extend the interaction surface (*16*). One example is illustrated by the structure of hepatocyte nuclear factor HNF-3γ bound to B-DNA (*17*) (Fig. 3A, right), where contacts include residues in two extended loops whose importance and spatial arrangement gave rise to the name "winged-helix" motif.

The mode of interaction of Zα with DNA (Fig. 3A, left) is markedly different from that of B-DNA binding HTH proteins, reflecting the fact that, unlike B-DNA, Z-DNA has no major groove and a very deep, nearly inaccessible minor groove. In Zα, recognition helix α3 is positioned on the outer surface of the DNA, with residues of the first two helical turns contacting the DNA. These residues are in the same positions as α3 residues used for B-DNA binding by the catabolite gene activator protein CAP and HNF-3γ (*17*) (Fig. 4B). In contrast to B-DNA binding HTH proteins with α/β topology, the first helix of the HTH motif in Zα is not involved in DNA contacts. Instead, the COOH-terminal β-hairpin contributes a second set of interactions. This β-hairpin is structurally well defined and is the region that deviates to the greatest extent from other HTH proteins with α/β topology. The cluster of highly conserved residues in the hairpin is specific to the Zα family (Fig. 4A) and is necessary for Z-DNA binding (*4, 11*). Unlike most structurally defined B-DNA binding HTH proteins, the interaction seen with Zα is conformation specific rather than sequence specific. The base contact to carbon 8 of G4 described above specifies the syn as opposed to the anti conformation of this base, but any base in the syn conformation at that position would expose a similar surface. These findings provide a structural basis for biochemical results, which describe a conformation specific binding behavior for the Zα domain (*6*).

The structural basis for sequence specific binding of B-DNA using the HTH motif is well established for many prokaryotic gene regulatory proteins and eukaryotic homeodomains [reviewed in (*18*)]. However, recently published HTH protein structures show marked variations of the originally described interaction with B-DNA. The endonuclease Fok I, the ribosomal protein L11, and the homeodomain protein bicoid are examples in which the HTH motif is used in a noncanonical way to bind B-DNA or even to interact specifically with RNA (*19*). Here, we describe the interaction between a HTH protein, Zα, with Z-DNA. Apparently, variations in the binding site of HTH proteins can result in very different substrate specificities.

A reduction in solvent-exposed surface area is thought to contribute significantly to the free energy of association (*16*). When Zα binds Z-DNA, 420 Å^2 of solvent-accessible protein surface area is lost (calculated with X-PLOR) (*20*), significantly less than in other specific protein-DNA complexes (*21*). However, there is extensive electrostatic and van der Waals complementarity, which may compensate in part (Fig. 3B, left), explaining the high affinity of Zα for Z-DNA (*22*). Furthermore, two Zα domains bind to the same Z-DNA duplex, albeit without contacts between the monomers, as shown in this crystal structure. In ADAR1, there is a second sequence, Zβ, which is very similar to Zα (Fig. 4A). These sequences are separated by a duplicated 49–amino acid module. The linker tethers the two regions together, and a bipartite Z-DNA binding domain, Zab, has been proposed (*7*). This would effectively double the interaction surface area. The coupling of subdomains to enhance DNA binding affinity and specificity has been seen in the bipartite OCT-1 and PAX-6 domains (*17*).

Z-DNA is formed transiently behind a moving RNA polymerase, stabilized by the

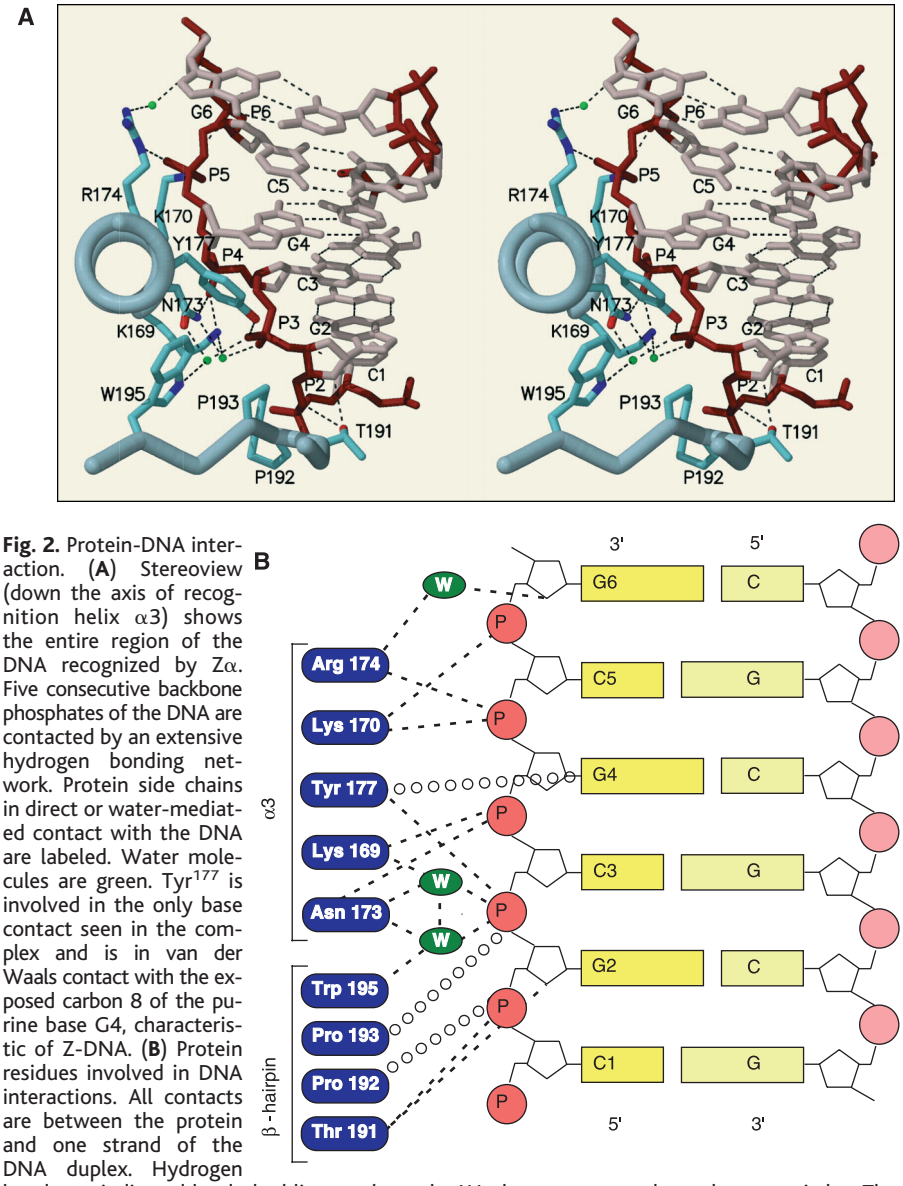

Fig. 2. Protein-DNA interaction. (**A**) Stereoview (down the axis of recognition helix α3) shows the entire region of the DNA recognized by Zα. Five consecutive backbone phosphates of the DNA are contacted by an extensive hydrogen bonding network. Protein side chains in direct or water-mediated contact with the DNA are labeled. Water molecules are green. Tyr^{177} is involved in the only base contact seen in the complex and is in van der Waals contact with the exposed carbon 8 of the purine base G4, characteristic of Z-DNA. (**B**) Protein residues involved in DNA interactions. All contacts are between the protein and one strand of the DNA duplex. Hydrogen bonds are indicated by dashed lines and van der Waals contacts are shown by open circles. Three water molecules in key positions within the protein-DNA interface are indicated by green ovals.

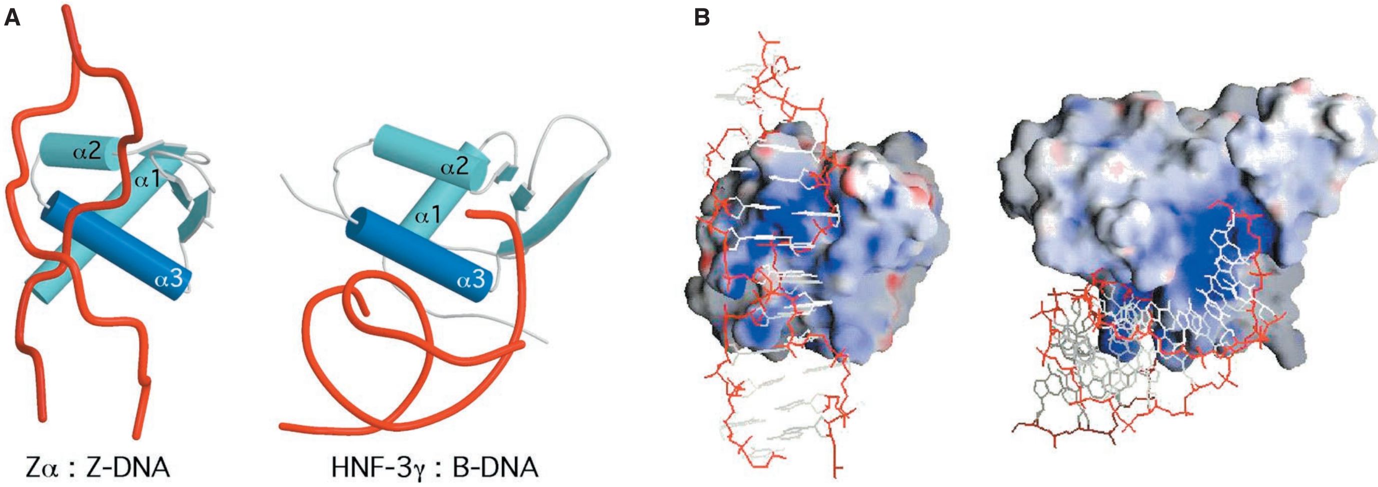

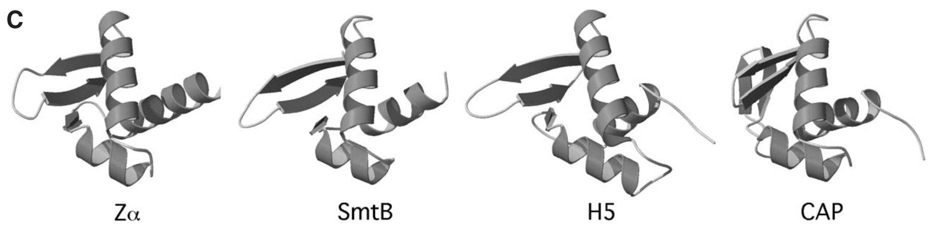

Fig. 3. Comparison with other HTH proteins. (**A**) Schematic of the Zα-DNA complex (left) compared with the HNF-3γ-DNA interaction (right) (*17*). Proteins are oriented with HTH units in the same orientation. The recognition helix α3 of the HTH motif is dark blue and the backbone trace of the DNA is red. The DNA axes are radically different because of the different "angle of attack" both proteins use to bind DNA. (**B**) Electrostatic surfaces of the proteins in the same orientation as in (A). Positive (blue) and negative (red) surface potentials are indicated. (**C**) Schematics showing the close similarity in topology of the Zα domain (left) and three members of the HTH family with α/β topology in order of increasing structural deviations from left to right: metallothionein repressor SmtB, globular domain of histone H5, and catabolite gene activator protein CAP (*13*).

```
                α1                              β1       α2                   α3             β2              β3
        134   140         150                               160                170         180               190         199
         :     :           :                                 :                  :           :                 :           :
hZα     SIYQDQEQRILKFLEEL------------GEGKATT----AHDLSGKL-------GTP-KKEINRVLYSLAKKGK-LQKEA-------GTPPLWKIAV

A
mZα     SISQSPEQKVLNRLEEL------------GEGKATT----AHVLAREL-------RIP-KRDINRILYSLEKKGK-LHRGR-------GKPPLWSLVP
rZα     SISQNPEQKVLNRLEEL------------GEGKATT----AYALAREL-------RTP-KKDINRILYSLERKGK-LHRGV-------GKPPLWSLVP
bZα     TISQDQEQRTLELLDEL------------GDGKATT----ARDLARKL-------QAP-KKDINRVLYSLAEKGK-LHQEA-------GSPPLWRATV
xZα1    TVSHDLLENNLLTFFKE------------IGTKTFT----AKALAWQF-------KVE-KKRINHFLYTFETKGL-LCRYP-------GTPPLWRVFS
xZα2     SVSRPLENILLTFFRG-----------QGDTQTFT----AKALAWQF-------KVK-KKHINYFLYKFQTKGL-LCKNS-------GTPPLWKISS
hZβ           MAEIKEKICDY-----------LFNVSDSS----ALNLAKNI-------GLTKARDINAVLIDMERQGD-VYRQG-------TTPPIWHLTD
mZβ           MAEIKEKICDY-----------LFNVSNSS----ALNLAKNI-------GLTKARDVTSVLIDLERQGD-VYRQG-------ATPPIWYLTD
rZβ           MAEIKEKICDY-----------LFNVSKSS----ALNLAKNI-------GLAKARDVNAVLIDLERQGD-VYREG-------ATPPIWYLTD
bZβ           MAEIKEKICDH-----------LFNVSSSS----ALNLAKNI-------GLTKARDVNAVLIDLERQGD-VYRQG-------TTPPIWYLTD
xZβ1          MAGNKEKVCEF-----------LYNSPPST----TLIIRKNV-------GISKLPELNQILNTLEKQGE-ACKAS-------TNPVKWTLTD
xZβ2           MATNSAKVCEF-----------LYNSPPST----PFIIRKNV-------GISKMPELTQILNTLEKQGE-ACKAS-------TNPVKWTLTA
E3L    MSKIYIDERSNAEIVCEA---------IKTIGIEGAT----AAQLTRQL-------NME-KREVNKALYDLQRSAM-VYSSD-------DIPPRWFMTT

B
SmtB   <44>DPNRLRLLSLLAR----------------selC----VGDLAQAI-------GVS-ESAVSHQLRSLRNLRL-VSYRk------qgrhVYYQL
H5     <27>  ySEMIAAAIRAEksrg------------GSS----RQSIQKYIkshykvghn-aDLQIKLSIRRLLAAGV-LKQTK-----gvgaSGSFRL
CAP   <137> dVTGRIAQTLLNLa-kqpdamthpdgmqikIT----RQEIGQIV-------GCS-RETVGRILKMLEDQNL-ISA-----------hGKTIVV
HNF3γ<123>  yISLITMAIQQApgk-------------mltlseiYQWIMDLF----pyyren-QQRWQNSIRHSLSfndcfvkvarspdkpgkgsywalh
```

Fig. 4. Sequence alignment of Zα homologs (Zα, Zβ, E3L) (**A**) and structurally related HTH proteins with α/β topology (SmtB, H5, CAP, HNF-3γ) (**B**). Numbering and secondary structural elements for Zα from human ADAR1 (hZα) are indicated above the sequences. Residues that contact Z-DNA in hZα are green if they are identical or chemically similar in the homologs; otherwise they are blue. In (B), residues situated in structurally equivalent positions between hZα and HTH proteins are in uppercase letters. DNA contacts with B-DNA (taken from published complex crystal structures) are red. The sequences are as follows: hZα, hZβ, ADAR1 *Homo sapiens*, accession number (acc) GenBank U18121; mZα, mZβ, ADAR1 *Mus musculus*, acc GenBank AF052506; rZα, rZβ, ADAR1 *Rattus norvegicus*, acc GenBank U18942; bZα, bZβ, ADAR1 *Bos taurus* (*5*); xZα1, xZβ1, dsRAD-1 *Xenopus laevis*, acc GenBank U88065; xZα2, xZβ2, dsRAD-2 *X. laevis*, acc GenBank U88066; E3L *Vaccinia virus* Western Reserve strain, acc GenBank S64006; SmtB, acc Protein Data Bank (PDB) 1SMT; CAP, acc PDB 1CGP; H5, acc PDB 1HST; HNF-3γ, acc Nucleic Acid Database PDT013.

negative supercoiling in its wake (*23*). ADAR1 has three dsRNA binding domains and it requires dsRNA to function. This dsRNA is frequently made in pre-mRNA by pairing intron and exon sequences; therefore, the editing must be completed before the introns are removed by the splicing machinery (*24*). It is postulated that the Z-DNA binding domain of ADAR1 targets the enzyme to actively transcribing genes (*25*), as they are the predominant sites for Z-DNA formation (*23*). It is likely that Z-DNA binding is evolutionarily maintained, because the residues that contact Z-DNA in Zα are well conserved within the family of Zα homo-

logs, including the second Z-DNA binding domain of ADAR1, Zβ, and the viral protein E3L (Fig. 4A).

The unique zigzag pattern of the sugar-phosphate backbone and the anti-syn alternation of the bases are characteristic of Z-DNA and distinguish it from other nucleic acid structures. The Zα domain has a tailored fit, which recognizes both features specifically. This binding can be generalized to other related left-handed Z-DNA binding HTH proteins and may provide a way to further explore the biological role(s) of Z-DNA.

References and Notes

1. A. H. Wang *et al*., *Nature* **282**, 680 (1979).
2. A. G. Herbert, J. R. Spitzner, K. Lowenhaupt, A. Rich, *Proc. Natl. Acad. Sci. U.S.A.* **90**, 3339 (1993); A. Herbert, K. Lowenhaupt, J. Spitzner, A. Rich, *ibid.* **92**, 7550 (1995).
3. A. G. Herbert and A. Rich, *Nucleic Acids Res.* **21**, 2669 (1993).
4. A. Herbert *et al*., *Proc. Natl. Acad. Sci. U.S.A.* **94**, 8421 (1997).
5. I. Berger *et al*., *Biochemistry* **37**, 13313 (1998).
6. A. Herbert *et al*., *Nucleic Acids Res.* **26**, 3486 (1998).
7. T. Schwartz *et al*., *J. Biol. Chem.* **274**, 2899 (1999).
8. The protein construct used here was originally named Za (*7*). It is structurally homogeneous, unlike other published Zα peptides. For simplicity, here we use the generic name Zα instead of Za.
9. Guanine nucleotides are in the syn conformation characteristic of Z-DNA, with C3′-endo sugar puckers. In contrast to crystals containing Z-DNA without protein, the DNA in this crystal does not form continuous helices; instead it is stacked 3′ to 3′ with the stacked molecules slightly displaced laterally. In pure DNA crystals the phosphate group in G4pC5 is seen in two alternate conformations, Z_I and Z_{II} [A. J. Wang *et al., Science* **211**, 171 (1981); R. V. Gessner, C. A. Frederick, G. J. Quigley, A. Rich, A. H. Wang, *J. Biol. Chem.* **264**, 7921 (1989)]. In the structure described here, this phosphate group is uniformly in the Z_I conformation as are all other phosphates at GpC steps. The Z_{II} conformation does not allow the interaction with Lys^{170}.
10. Two complexes (I, II) are related by a noncrystallographic twofold axis, and the third (III) resides on a crystallographic dyad. Some amino acids at the NH_2- and COOH-termini of the protein are disordered. The structure is defined for residues 134 to 198 of the Zα monomer in complex I, 136 to 199 in complex II, and 134 to 199 in complex III. The DNA structure is well resolved except for the 5′-dT overhang, which appears to be disordered.
11. M. Schade, C. J. Turner, K. Lowenhaupt, A. Rich, A. Herbert, *EMBO J.* **18**, 470 (1999).
12. S. K. Burley and G. A. Petsko, *Adv. Prot. Chem.* **39**, 125 (1988).
13. Single-letter abbreviations for amino acid residues are as follows: A, Ala; C, Cys; D, Asp; E, Glu; F, Phe; G, Gly; H, His; I, Ile; K, Lys; L, Leu; M, Met; N, Asn; P, Pro; Q, Gln; R, Arg; S, Ser; T, Thr; V, Val; W, Trp; and Y, Tyr.
14. Rmsd is 0.93 Å between complex I and II, 1.07 Å between complex II and III, and 0.76 Å between complex I and III, including all protein and DNA atoms, even though the three complexes were built and refined entirely independently.
15. When the Zα domain is superimposed on other proteins in the family, the similarity is most striking with the metallothionein transcriptional repressor SmtB (*17*) (rmsd 44 C^α atoms 0.79 Å), the catabolite gene activator protein CAP (*17*) (rmsd 43 C^α atoms 0.94 Å), and the related winged-helix class of proteins, such as hepatocyte nuclear factor HNF-3γ (*17*) (rmsd 30 C^α atoms 2.36 Å) and histone H5 (*17*) (rmsd 39 C^α atoms 1.28 Å).
16. D. M. J. Lilley, *DNA-Protein: Structural Interactions* (Oxford Univ. Press, Oxford, 1995).
17. Structures: HNF-3γ [K. L. Clark, E. D. Halay, E. Lai, S. K. Burley, *Nature* **364**, 412 (1993)], SmtB [W. J. Cook, S. R. Kar, K. B. Taylor, L. M. Hall, *J. Mol. Biol.* **275**, 337 (1998)], CAP [S. C. Schultz, G. C. Shields, T. A. Steitz, *Science* **253**, 1001 (1991)], H5 [V. Ramakrishnan, J. T. Finch, V. Graziano, P. L. Lee, R. M. Sweet, *Nature* **362**, 219 (1993)], OCT-1 [J. D. Klemm, M. A. Rould, R. Aurora, W. Herr, C. O. Pabo, *Cell* **77**, 21 (1994)], and PAX-6 [H. E. Xu *et al., Genes Dev.*, in press].
18. S. C. Harrison and A. K. Aggarwal, *Annu. Rev. Biochem.* **59**, 933 (1990); C. O. Pabo and R. T. Sauer, *ibid.* **61**, 1053 (1992).
19. D. E. Draper and L. P. Reynaldo, *Nucleic Acids Res.* **27**, 381 (1999); S. K. Chan and G. Struhl, *Nature* **388**, 634 (1997); D. A. Wah, J. A. Hirsch, L. F. Dorner, I. Schildkraut, A. K. Aggarwal, *ibid.*, p. 97.
20. Program tools: X-PLOR [A. T. Brünger, *X-PLOR Version 3.1. A System for X-ray Crystallography and NMR* (Yale Univ. Press, New Haven, CT, 1992)], HKL package [Z. Otwinowski and W. Minor, *Methods Enzymol.* **276A**, 307 (1997)], SOLVE [T. C. Terwilliger and J. Berendzen, *Acta Crystallogr.* **D52**, 749 (1996)], DM [K. Cowtan and P. Main, *ibid.*, p. 43 (1996)], and Procheck [A. L. Morris, M. W. MacArthur, E. G. Hutchinson, J. M. Thornton, *Proteins* **12**, 345 (1992)].
21. For example, in the engrailed homeodomain-DNA complex, 960 $Å^2$ of protein surface area is lost upon binding [E. Fraenkel, M. A. Rould, K. A. Chambers, C. O. Pabo, *J. Mol. Biol.* **284**, 351 (1998)].
22. The dissociation constant for Zα bound to a 6-bp DNA duplex $d(CGCGCG)_2$ is 30 nM, as determined by ultracentrifugation (M. Schade *et al*., unpublished data).
23. L. F. Liu and J. C. Wang, *Proc. Natl. Acad. Sci. U.S.A.* **84**, 7024 (1987); B. Wittig, T. Dorbic, A. Rich, *ibid.* **88**, 2259 (1991); B. Wittig, S. Wölfl, T. Dorbic, W. Vahrson, A. Rich, *EMBO J.* **11**, 4653 (1992).
24. S. Maas, T. Melcher, P. H. Seeburg, *Curr. Opin. Cell Biol.* **9**, 343 (1997).
25. A. Herbert and A. Rich, *J. Biol. Chem.* **271**, 11595 (1996).
26. T. Schwartz *et al*., *Acta Crystallogr.*, in press.
27. Figures were made with MOLSCRIPT (Figs. 1 and 2A) [P. J. Kraulis, *J. Appl. Crstallogr.* **24**, 946 (1991)], Bobscript (Fig. 3A) [R. M. Esnouf, *J. Mol. Graphics* **15**, 132 (1997)], and RASTER-3D [E. A. Merritt and E. P. Murphy, *Acta Crystallogr. D* **50**, 869 (1994)]. Figure 3B was made with GRASP [A. Nicholls, K. A. Sharp, B. Honig, *Proteins Struct. Funct. Genet.* **11**, 281 (1991)].

28. Supported by grants from the National Institutes of Health and the National Science Foundation and by a fellowship from the German Academic Exchange Service (DAAD) to T.S. Coordinates for the crystal structure have been deposited in the Protein Data Bank (accession code 1QBJ).

5 March 1999; accepted 29 April 1999

Specific Coupling of NMDA Receptor Activation to Nitric Oxide Neurotoxicity by PSD-95 Protein

Rita Sattler,[1] Zhigang Xiong,[2] Wei-Yang Lu,[2] Mathias Hafner,[3] John F. MacDonald,[2] Michael Tymianski[1]*

The efficiency with which *N*-methyl-D-aspartate receptors (NMDARs) trigger intracellular signaling pathways governs neuronal plasticity, development, senescence, and disease. In cultured cortical neurons, suppressing the expression of the NMDAR scaffolding protein PSD-95 (postsynaptic density–95) selectively attenuated excitotoxicity triggered via NMDARs, but not by other glutamate or calcium ion (Ca^{2+}) channels. NMDAR function was unaffected, because receptor expression, NMDA currents, and $^{45}Ca^{2+}$ loading were unchanged. Suppressing PSD-95 blocked Ca^{2+}-activated nitric oxide production by NMDARs selectively, without affecting neuronal nitric oxide synthase expression or function. Thus, PSD-95 is required for efficient coupling of NMDAR activity to nitric oxide toxicity, and imparts specificity to excitotoxic Ca^{2+} signaling.

Calcium influx through NMDARs plays key roles in synaptic transmission, neuronal development, and plasticity (*1*). Excessive Ca influx triggers excitotoxicity (*2*), damaging neurons in diverse neurological disorders (*3*). Rapid Ca^{2+}-dependent neurotoxicity is triggered most efficiently when Ca^{2+} influx occurs through NMDARs, and cannot be reproduced by loading neurons with equivalent quantities of Ca^{2+} through non-NMDARs or voltage-sensitive Ca^{2+} channels (VSCCs) (*4*). This suggests that Ca^{2+} influx through NMDAR channels is functionally coupled to neurotoxic signaling pathways.

We hypothesized that lethal Ca^{2+} signaling by NMDARs is determined by the molecules with which they interact. The NR2 NMDAR subunits bind to PSD-95/SAP90 (*5*), chapsyn-110/PSD-93, and other members of the membrane-associated guanylate

[1]Toronto Western Hospital, University of Toronto, Lab 11-416, 399 Bathurst Street, Toronto, Ontario M5T 2S8, Canada. [2]Department of Physiology, University of Toronto, Toronto, Ontario M5G 1X8, Canada. [3]Mannheim University of Applied Sciences, 68163 Mannheim, Germany.

*To whom correspondence should be addressed. E-mail: mike_t@playfair.utoronto.ca